Effect of Electron Cyclotron Current Drive on the Ion Temperature in the Plasma Core Region of the Large Helical Device

Yasuo YOSHIMURA[1)], Akira EJIRI[2)], Ryosuke SEKI[1)], Ryuichi SAKAMOTO[1,3)], Kenichi NAGAOKA[1,4)], Takashi SHIMOZUMA[1)], Hiroe IGAMI[1)], Hiromi TAKAHASHI[1,3)], Toru I. TSUJIMURA[1)], Felix WARMER[5)], Kota YANAGIHARA[4)], Yuki GOTO[4)], Katsumi IDA[1,3)], Mikiro YOSHINUMA[1,3)], Tatsuya KOBAYASHI[1,3)], Shin KUBO[1,4)], Masaki OSAKABE[1,3)], Tomohiro MORISAKI[1,3)] and the LHD Experiment Group

[1)]*National Institute for Fusion Science, National Institutes of Natural Sciences, Toki, Gifu 509-5292, Japan*
[2)]*The University of Tokyo, Graduate School of Frontier Sciences, Kashiwa, Chiba 277-8561, Japan*
[3)]*SOKENDAI (The Graduate University for Advanced Studies), Department of Fusion Science, Toki, Gifu 509-5292, Japan*
[4)]*Nagoya University, Graduate School of Engineering, Nagoya, Aichi 464-8603, Japan*
[5)]*Max Planck Institute for Plasma Physics, EURATOM Association, D-17491 Greifswald, Germany*

(Received 12 December 2017 / Accepted 29 October 2018)

An indirect effect of the electron cyclotron current drive (ECCD) on the ion temperature in the plasma core region was observed in the Large Helical Device. The reference (no ECCD) discharge with a central ion temperature T_{i0} of ~3.0 keV is operated by a standard high ion temperature discharge procedure. To investigate the ECCD effect, a co- or counter-ECCD was applied to the reference discharge, and was turned off immediately before the T_{i0} peaked in the reference discharge. In the co-ECCD and counter-ECCD applications, the T_{i0} temporarily increased and decreased by ~0.5 keV from T_{i0} in the reference discharge, respectively. The mechanism of this phenomenon is presently unclear, but may be exploited as a practical knob for controlling the central ion temperature.

Keywords: electron cyclotron current drive (ECCD), ion temperature, Large Helical Device (LHD)

DOI: 10.1585/pfr.13.1402124

1. Introduction

Achievement of central ion temperature T_{i0} of higher than 10 keV is one of the target figures of the Large Helical Device (LHD) project [1, 2]. In both tokamaks [3] and stellarators [4], the empirical scaling laws of the energy confinement time positively depend on the plasma current I_p or the rotational transform $\iota/2\pi = t$. Similarly, in the LHD, discharges with co-dominant neutral beam injections (NBIs) are empirically known to favor higher T_{i0} than those with counter-dominant NBIs. These phenomena may be interpreted as a modified t profile, including magnetic island formation or stochastization of the magnetic field [5]. Thus, it is expected that T_{i0} can be enhanced by controlling I_p and/or t. This paper presents the experimental results of varying I_p and t by application of the on-axis co- and counter-ECCDs.

In past LHD experiments, simultaneous application of electron cyclotron heating (ECH) or ECCD around the timing of the high T_{i0} state in the reference discharge (without ECH or ECCD) resulted in the decreases of the ion temperature gradient ∇T_i and T_{i0}, although the central electron temperature T_{e0} became higher than T_{i0} [6]. Thus, the effects of I_p and t on T_{i0} must be investigated in another operational scenario of ECH or ECCD.

Based on these observations, we attempted to increase the T_{i0} in the LHD by experimentally investigating the effect of ECCD on T_i. To separate the T_{i0} variation into that due to T_e variation and that due to the I_p and/or t variation, we turned off the ECCD immediately before the start of an NBI, when the highest T_{i0} is expected. Owing to the relatively long time constant of current redistribution and the relatively short energy confinement time, we can temporarily realize a state with the I_p and/or t effect, but without the T_e effect.

The remainder of this paper is organized as follows. Section 2 briefly describes the LHD and its heating devices, and Sec. 3 describes the experimental results obtained in the high T_i discharge with the ECCD. The results are summarized in Sec. 4.

2. LHD and Its Heating Devices

The LHD is a helical device with a toroidal period number $m = 10$ and polarity $l = 2$. The magnetic field configuration, including the rotational transform for the plasma confinement, can be generated only by external superconducting magnets: a pair of helical coils and three pairs of poloidal coils. The magnetic axis position R_{ax} can

author's e-mail: yoshimura.yasuo@nifs.ac.jp

be varied from 3.42 to 4.1 m. In the discharges described in this paper, R_{ax} was set at a typical position (3.6 m), and the magnetic field B_t along the magnetic axis (averaged over the toroidal direction) was set to 2.75 T.

The main components of the ECH system on the LHD are five high-power (> 1 MW each) gyrotrons, three oscillating at 77 GHz (the fundamental resonance frequency in the 2.75 T magnetic field), and two oscillating at 154 GHz (the 2nd harmonic resonance in 2.75 T). The launching part of the ECH/ECCD system was upgraded to 4-beam antenna systems in the 2-O horizontal port [7]. Each antenna system in the 2-O port has a wide controllable range of the electron cyclotron (EC)-wave beam direction for power-deposition control and ECCD.

The NBI system consists of three tangentially injecting negative ion source NBIs (#1, #2, and #3) and two perpendicularly injecting positive ion source NBIs (#4 and #5) [8]. In the magnetic field configuration of the discharges in this paper, NBI#1 and NBI#3 were co-injected such that the NB-driven current increased the ι, while NBI#2 was counter-injected to decrease the ι. The injection energies/port-through powers of the NBIs were set as follows: 183 keV/5.4 MW for NBI#1, 172 keV/4.5 MW for NBI#2, 177 keV/2.6 MW for NBI#3, 39 keV/3.0 MW for NBI#4, and 44 keV/4.2 MW for NBI#5. To measure the T_i profile by charge exchange spectroscopy (CXS) [9], we modulated the power of NBI#4 by 80 ms-on and 20 ms-off sequence. The rotational transform profiles were diagnosed by motional Stark effect (MSE) measurements [10, 11].

3. Application of ECCD to High Ion Temperature Discharges in LHD

The time sequence of the standard high T_i discharges in the LHD [6, 8] is as follows. An initial plasma is generated by a short pulse (t = 3 - 3.3 s) EC-wave power injection. This plasma is heated and sustained until t = 5.5 s by the perpendicular NBI#5. The tangential NBIs (NBI#1, #2, and #3) are applied from t = 4 s. Finally, when the perpendicular NBI#4 is applied from t = 4.5 s, the total NBI power and T_{i0} are maximized. Immediately before the injection of NBI#4, a carbon pellet is injected. After a rapid increase of the electron density caused by carbon pellet injection, the highest T_{i0} is temporarily reached during the decay phase of the density. Even without the carbon pellet, NBI#4 injection achieves a high T_{i0} with a similar time evolution, but the obtained T_{i0} is lower than in the pellet case. The discharges in this paper were performed in the absence of carbon pellets and wall conditioning. Substantial wall conditioning using ion cyclotron heating (ICH) and/or ECH is also required to boost the T_{i0} [12].

To search for a positive effect of ECCD on T_i, we applied co- and counter-ECCDs to the above-mentioned high T_i discharges. As the time constants of T_e and I_p are on the order of 0.1 s and more than a few seconds respectively,

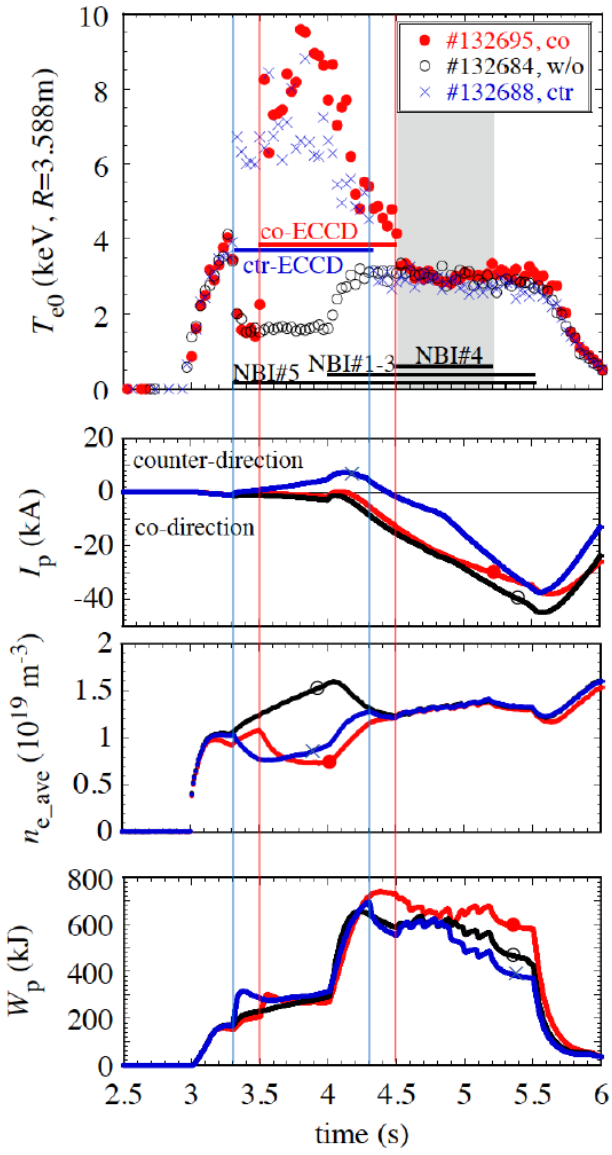

Fig. 1 Time evolutions of plasma parameters in the three typical discharges: applications of co-ECCD (#132695, red closed circles), counter-ECCD (#132688, blue crosses), and no ECCD (#132684, black open circles). Top to bottom: central electron temperature, plasma current, line-averaged electron density, and plasma stored energy. The top panel also indicates the timings of the EC-wave and NB injections.

the ECCD was turned off immediately before starting the NBI#4 injection. Thus, maintaining the clear I_p difference between the applications of co- and counter-ECCDs, the electron temperature was decreased to the non-ECCD level at the timing of the NBI#4 injection. Figure 1 shows the waveforms in this operational scenario. Shown are the time evolutions of T_{e0}, I_p, the line-averaged electron density n_{e_ave}, and the plasma stored energy W_p in the three discharges (co- and counter-ECCD applications and no ECCD). In the case without ECCD, the electron temperature dropped to ~1.5 keV at t = 3.3 s, when the initial

EC-wave power injection was turned off, but was increased by NBIs#1 - 3 at t = 4 s. The working gas of the NBIs was hydrogen, with no additional gas puffing to generate and sustain plasmas in this density range. Thus, most of the ions were hydrogen (> 90%) and the remainder were mostly helium.

Both co- and counter-ECCDs heat the electrons and reduce their density. To observe the effects of I_p and/or ι, the ECCDs were turned off at t = 4.3 s or 4.5 s and the T_e and n_{e_ave} were adjusted to similar values at t > 4.5 s. The counter-ECCD used all four EC-wave beams with a total power of ~4 MW from the 2-O horizontal port, but (owing to technical limitation) the co-ECCD was limited to three EC-wave beams with a total power of ~3 MW. The application time periods of the co- and counter-ECCDs were also shifted by 0.2 s. However, these differences in the power and period are not essential, because the ion temperatures at the start of the NBI#4 injection are similar, as shown below. In the no ECCD and counter-ECCD cases, the W_p decreased at t > ~4.85 s due to break down in the NBI#2 operations at 4.85 s in #132688 and at 4.93 s in #132684. When the ECCDs were applied until t = 4.3 s or 4.5 s, the ι profile at t = 4.6 s was modified from that of the reference (no ECCD) case. As shown in Fig. 2, the ι profile in the plasma core region was increased/decreased by the co-/counter-ECCD application, as expected.

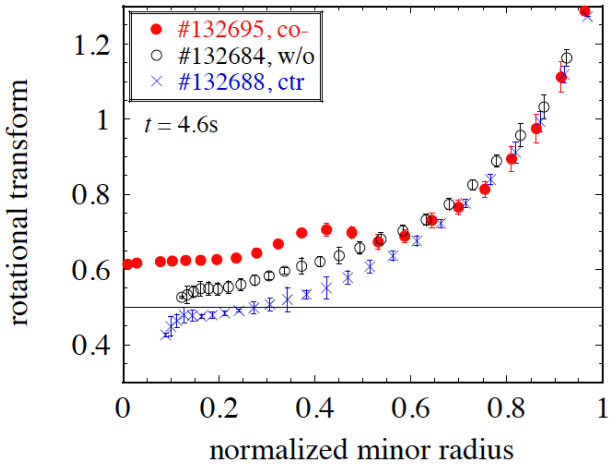

Fig. 2 Radial profiles of rotational transform diagnosed by MSE measurements at t = 4.6 s in the co-ECCD, counter-ECCD, and no ECCD discharges.

As the result of the application of ECCDs to the plasmas sustained based on the procedure for standard high ion temperature discharges, the ion temperature in the plasma core region was clearly modified (see Figs. 3 (a) and 4). In both the T_i profiles at t = 4.67 s in Fig. 3 (a) and the time evolutions of T_{i0} in Fig. 4, the T_{i0} deviated from the reference by ~0.5 keV in the plasma core region, although the increment was unsteady. The T_{i0} increment caused by the NBI#4 application was higher in the co-ECCD case than in the reference discharge without ECCD. In the counter-ECCD case, the NBI#4 injection did not raise the T_{i0}. The experimental results of T_{i0} and ι can be interpreted as the development of magnetic islands or stochastization of the magnetic field in the plasma core region. As shown in Fig. 2, ι was lower than 0.5 at ρ < 0.3 in the counter-ECCD case, and (although measured data were unavailable) appeared to be 0.5 at ρ < ~0.1 in the absence of ECCD. On the other hand, in the co-ECCD case, ι exceeded 0.5 even at the plasma center. Thus, magnetic islands or stochastic magnetic fields related to the existence of the rational surface of ι = 0.5, and their extension into the plasma core region, can be a cause of the degradation of the T_i and its affected width in the counter-ECCD and no ECCD cases. However, neither ECCD application caused a noticeable difference from the reference T_e profile in Fig. 3 (b), although magnetic islands or stochastic magnetic fields (if present) should also affect the T_e profiles. Therefore, the causal relationship between the T_{i0} and ι variations cannot

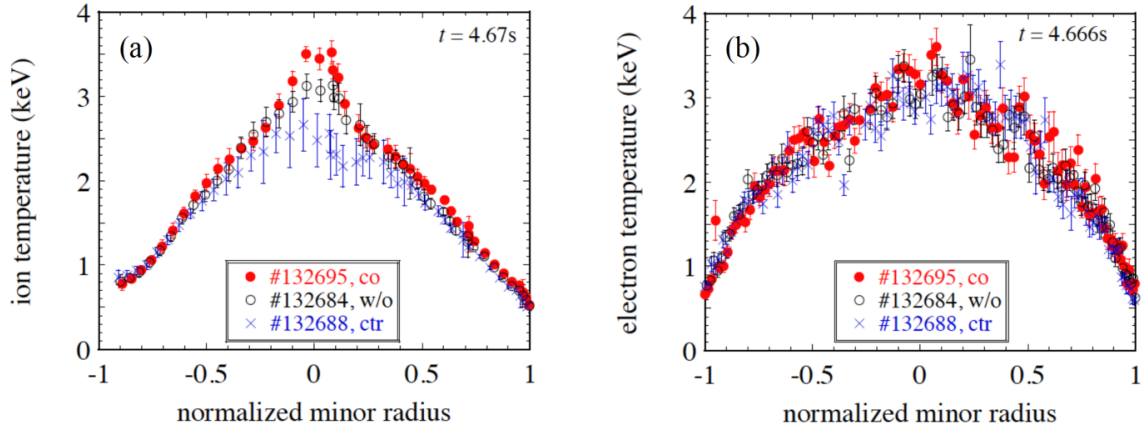

Fig. 3 (a): Radial profiles of ion temperature diagnosed by CXS measurements at t = 4.67 s in the co-ECCD, counter-ECCD, and no ECCD discharges. The results were obtained by spatial averaging of each set of three neighboring data points in the original data. (b): Radial profiles of electron temperature diagnosed by Thomson scattering measurements at t = 4.666 s.

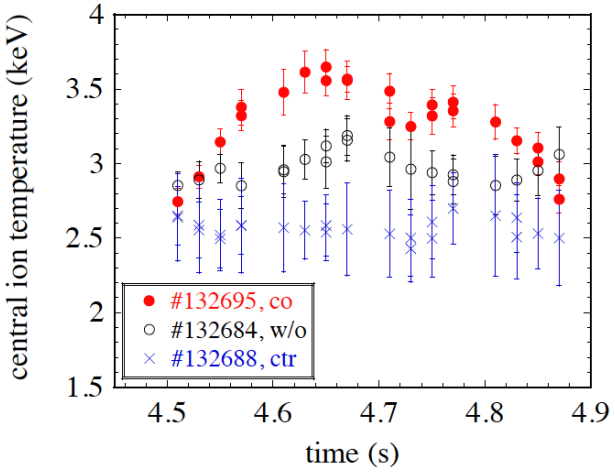

Fig. 4 Time evolutions of central ion temperature in the co-ECCD, counter-ECCD, and no ECCD discharges. The results were obtained by temporal averaging of each set of three neighboring data points in the original data.

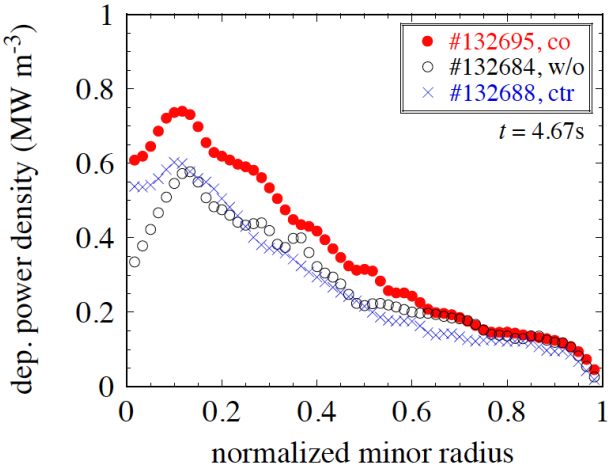

Fig. 5 Radial profiles of NBI deposition power density imparted to the ions, analyzed by TR-snap code at $t = 4.67$ s in the co-ECCD, counter-ECCD, and no ECCD discharges.

be clarified by the current data.

We next considered the total deposition power and central power density of the NBIs on the ions. The central heating power density should exert a stronger influence on T_{i0} than the total heating power imparted to the ions. The NBI deposition powers at $t = 4.67$ s were calculated by TR-snap code [13], a transport-coefficient evaluation tool based on power balance. The total deposition powers imparted to the ions and electrons by the five NBIs were 6.42 MW and 6.67 MW respectively in the co-ECCD discharge (shot #132695), 5.62 MW and 6.14 MW respectively in the absence of ECCD discharge (shot #132684), and 4.94 MW and 6.32 MW respectively in the counter-ECCD discharge (shot #132688). Note that the power imparted to the ions decreased in the order 6.42 MW (co-ECCD) > 5.62 MW (no ECCD) > 4.94 MW (counter-ECCD), consistent with the order of decreasing T_{i0}s. Note also that the equipartition powers from the electrons to ions were negligibly small (only 0.3 MW), owing to the small difference between the ion and electron temperatures (see Fig. 3). On the other hand, the central ($\rho < \sim 0.1$) ion heating power densities decreased in the order ~ 0.7 MW m^{-3} (co-ECCD) > ~ 0.55 MW m^{-3} (counter-ECCD) > ~ 0.45 MW m^{-3} (no ECCD) (see Fig. 5), inconsistent with the decreasing order of T_{i0}s. Thus, the differences in the calculated NBI deposition power densities in the plasma center region cannot explain the variations of T_{i0} in the three ECCD discharge cases (co-, counter-, and reference).

Further studies are required to identify the mechanism of the change in T_{i0}. Although the reasons are unknown at present, ECCD evidently affects the T_{i0}, indicating that applying an on-axis ECCD is effective for controlling the ion temperature in the plasma core region.

4. Summary and Conclusion

An indirect effect of ECCD on the ion temperature in the plasma core region was observed in the LHD experiment. Based on the standard procedure of high ion temperature discharges, an on-axis co-ECCD was applied until just before the timing of the highest ion temperature in the reference discharge. With the co-ECCD application, the T_{i0} was raised to ~ 0.5 keV above T_{i0} in the reference discharge, although the increment was unsteady. On the contrary, the counter-ECCD lowered T_{i0} by ~ 0.5 keV from that of the reference discharge. At present, investigations of both the rotational transform and calculated NBI deposition power density provide no satisfactory interpretation of the ion temperature evolution. Possible formation of magnetic islands or stochastization of the magnetic field caused by changes in the rotational transform can explain the changes in the T_i profile, but cannot explain the invariance of the T_e profile. Moreover, the order in which the magnitudes of the calculated NBI deposition power densities decreased in the plasma center region of the three cases (co-ECCD, counter-ECCD and reference) disagreed with that of the T_{i0}s. To elucidate the physical mechanism of this phenomenon, which is related to the plasma current and/or rotational transform, or to other unnoticed state/parameters such as modification of the magnetic field structure and the induced toroidal electric field, should be experimentally and theoretically investigated in future studies.

Acknowledgments

The authors would like to express their gratitude to the LHD Experiment Group for performing the LHD experiments. This work was supported by the NIFS grants ULRR701 and collaboration research programs of NIFS (NIFS15KLPR030). The authors would like to thank

Enago (www.enago.jp) for the English language review.

[1] Y. Takeiri *et al*., Nucl. Fusion **57**, 102023 (2017).
[2] K. Ida *et al*., Nucl. Fusion **55**, 104018 (2015).
[3] ITER Physics Basis Editors, Nucl. Fusion **39**, 2137 (1999).
[4] H. Yamada *et al*., Nucl. Fusion **45**, 1684 (2005).
[5] K. Ida *et al*., Plasma Phys. Control. Fusion **57**, 014036 (2015).
[6] K. Nagaoka *et al*., Nucl. Fusion **55**, 113020 (2015).
[7] Y. Yoshimura *et al*., Plasma Fusion Res. **11**, 2402036 (2016).
[8] Y. Takeiri *et al*., Plasma Fusion Res. **10**, 1402001 (2015).
[9] M. Yoshinuma *et al*., Fusion Sci. Technol. **58**, 375 (2010).
[10] K. Ida *et al*., Fusion Sci. Technol. **58**, 383 (2010).
[11] T.J. Dobbins *et al*., Rev. Sci. Instrum. **88**, 093518 (2017).
[12] H. Takahashi *et al*., J. Nucl. Mater. **463**, 337 (2015).
[13] R. Seki *et al*., Plasma Fusion Res. **6**, 2402081 (2011).